

A phenomenological model for sonic crystals based on artificial neural networks

E. Fuster-García, V. Romero-García, and Juan V. Sánchez Pérez^{a)}

Grupo de Acústica Arquitectónica y del Medio Ambiente and Departamento de Física Aplicada, ETSICCP, UPV, Cno. de Vera s/n, 46020 Valencia, Spain

L. M. García-Raffi and Enrique A. Sánchez Pérez

Instituto de Matemática Pura y Aplicada and Departamento de Matemática Aplicada, ETSICCP, UPV, Cno. de Vera s/n, 46020 Valencia, Spain

(Received 13 January 2006; revised 30 May 2006; accepted 1 June 2006)

A phenomenological model that simulates the acoustic attenuation behavior of sonic crystals is developed in this paper. The input of the model is a set of parameters that characterizes each experimental setup, and the output is a simulation of the associated attenuation spectrum. The model consists of a combination of a multiresolution analysis based on wavelet functions and a set of artificial neural networks. An optimized coupling of these tools allows us to drastically reduce the experimental data needed, and to obtain a fast computational model that can be used for technological purposes. © 2006 Acoustical Society of America. [DOI: 10.1121/1.2217127]

PACS number(s): 43.20.Fn, 43.60.Np [KA]

Pages: 636–641

I. INTRODUCTION

Sonic crystals (SCs) are structures formed by a periodic array of acoustic scatterers embedded in a homogeneous material, with strong modulation of the elastic constants between the scatterers and the surrounding materials. The periodicity in these materials results in the appearance of sonic band gaps, a range of frequencies for which sound propagation is forbidden inside the crystal. These stop bands have induced several application proposals, such as acoustic filters and shield devices.^{1–6}

In recent years, a great experimental and theoretical effort has been made in order to improve the knowledge of the acoustical properties of these systems. Theoretical simulation programs have been developed to predict the behavior of such structures. Some of them calculate the acoustic band structure of infinite crystal using the plane-wave expansion method.^{7,8} Other approaches, based on a variational method⁹ and a Korrington-Khon-Rostoker method,¹⁰ have been developed. Also, finite systems have been studied using the transfer-matrix method^{4,11} and multiple scattering theory^{12–14} (MST). Experimental measurements, under controlled and outdoor conditions, have been performed² in the audible range.

It has been observed that the acoustic attenuation spectra produced by SCs depend not only on the lattice constant but also on the filling factor, type of array, sound incidence angle, and measure distance. Small variations on them can produce big changes in the shape and position of the attenuation peaks in the spectrum.⁹

Moreover, although it has been proved that the simulation programs provide satisfactory results, there is still a gap between theoretical and experimental spectra. Theoretical models give us qualitative information about the shape and

variation of the attenuation peaks, but this information is not as complete as is required for the technological development of the SCs. In this sense, it would be interesting to perform models based on experimental data that have been obtained in situations that are close to the use of SCs, such as acoustic filters or shield devices. Our paper presents this type of model. It is based on the interplay between two well-known mathematical techniques: Multiresolution analysis (MRA),^{15–17} and artificial neural networks (ANNs).^{18–20} Our procedure consists of a four-step scheme. First, we have to measure attenuation spectra corresponding to different values of the parameters defining both the crystal and the experimental conditions of the measurement (SC setups). Second, in order to present the experimental information to the ANN in a compressed and arranged format, we analyze attenuation spectra with MRA based on wavelet transform. In the third step, we train a set of neural networks with the experimental data. The objective is that ANNs correlate pairs formed by a vector of n parameters, that define the SC setup and the corresponding experimental attenuation spectrum. This correlation will allow us to simulate attenuation spectra. The fourth step consists of a test of the model; comparing simulated with experimental spectra specifically preserved as samples for this purpose.

Note that the conditions under which the model works consider only SC setups defined by a vector of parameters whose values lie inside the range of values used in the construction of the model.

We present results of our model for a well-known two-dimensional SCs configuration, formed by hollow aluminium cylinders rods arranged in triangular cells embedded in air,⁹ in order to allow the comparison between the results obtained with our model and the theoretical calculation using MST.

^{a)}Electronic mail: jusanc@fis.upv.es

II. MATHEMATICAL APPROACH

The core of our model is composed of a set of ANNs that compute the correlation between vectors of parameters corresponding to different SC setups and the associated experimental spectra. To achieve this objective, we perform a supervised training of networks with pairs formed by a vector and an associated spectrum. These spectra are defined by a great number of channels (512, in our case) to obtain a good resolution. If raw spectra were used, a complex ANN structure would be needed, and a great number of experimental samples would be necessary to train it. A natural way to overcome this problem is to try to characterize the attenuation peaks in spectra by a few number of parameters. We can try to use classical spectroscopic techniques for a systematic analysis of peaks, such as, fitting peaks with respect to a well-known base of functions to obtain a characterization of them (centroid, width, tail, etc.). But, as we have mentioned in Sec. I, the nature of the physical processes involved produces a great variety of attenuation peak shapes. Consequently, these classical techniques are not appropriate for this purpose. Therefore, we have decided to use another mathematical tool for analyzing attenuation spectra; the MRA based on the wavelet transform.¹⁵ Moreover, the MRA allows us to present experimental spectra to the network in a very compressed and arranged format, which drastically reduces the number of degrees of freedom of our model and the error associated to the simulated spectra. The MRA uses the properties of wavelets basis to decompose the signal into a sequence of different resolution levels. Roughly speaking, this analysis allows us to distinguish between the spectrum's tendencies and fluctuations.¹⁶ This property of MRA facilitates both data compression—via the deletion of the coefficients of the nonrelevant levels easily—and also filtering data—which establishes suitable thresholds for the value of the coefficients. For these reasons, MRA turns out to be extremely effective for the systematization of the analysis of the peaks in acoustic attenuation spectra.

An ANN is composed of many simple nonlinear computational elements; operating in parallel and densely interconnected. Several interconnected neurons organized in layers can form an ANN. In this work, we have used a feedforward network topology, where the data processing can extend over multiple layers of neurons but no feedback connections are present (connections extending from outputs of neurons to inputs of neurons in the same layer or previous layers).

In order to set up the ANN for a specific use, a training process and a learning process are needed. The training process consists of feeding the ANN with teaching patterns, and letting it change its weights and bias according to some learning rule. The algorithm used in this work for training is the *Levenberg-Marquardt optimization algorithm*.²⁰ The learning rules are methods of deriving the next changes that might be made in a network. In our case, we use the learning function *Gradient descent with momentum weight and bias*.¹⁹

III. DEVELOPMENT OF THE MODEL

As we have just mentioned, our model is constructed following a four-step procedure indicated in Fig. 1.

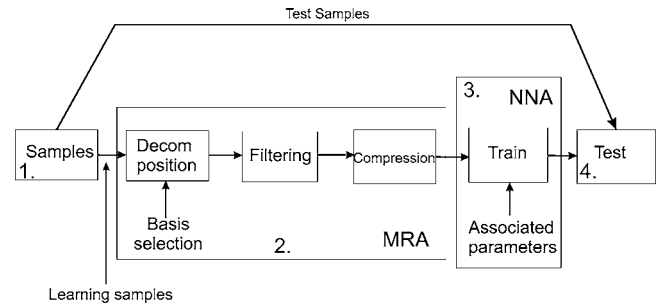


FIG. 1. Diagram of procedure for building the model.

A. Experimental data set

The first step consists of obtaining a significant set of experimental data corresponding to a region of the parameters space where we want to use the model.

The experiments have been performed in an anechoic chamber of $8 \times 6 \times 3 \text{ m}^3$. We use a sound source with a speaker placed at the focus of a parabolic reflector to obtain a plane wave. However, since the dimension of the chamber is not much larger than the SC size, sound waves are not full plane waves when the wavefronts reach the SC. The SCs are built up by hanging cylindrical rods on a frame with triangular symmetry. The frame can rotate around the vertical axis, so one can explore any direction of the wave vector perpendicular to the cylinder axis. Here, we use 1 m length hollow aluminium rods. The points of measurements are always placed on the axis defined by the center of the SC and the source. In these points, the continuous white noise emitted by the source is recorded by a microphone with and without SC (insertion loss). The attenuation spectrum is obtained from the difference between the two signals. A dual-channel signal analyzer (type *B&K 2148*) has been used throughout all experiments. The analyzer makes the fast Fourier transform (FFT) of the data and produces the corresponding spectrum with a resolution of 8 Hz. A range from 800 to 4888 Hz is analyzed, and a total of 512 channels have been taken to generate a spectrum.

We have assigned a vector of five parameters (input vector) to every SC setup. These parameters are: Incidence angle, cylinders radii, lattice spacing, distance from the point of measurement to the center of the structure, and number of rows of the SC.

The incidence angle (θ), calculated between the direction of the wave vector (\mathbf{k}) (see Fig. 2) and the symmetry axis of the crystal, ranges from 0° to 30° (5° step). The values of the radii of used scatterers (r) are: 0.8, 1, 1.25, 1.5,

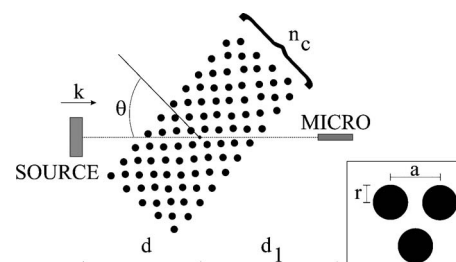


FIG. 2. Definition of parameters used for characterizing every SC setup.

1.75, and 2 cm. The lattice constant (a) can take two values: 6.35 and 12.7 cm. The distance between the center of the structure and the point of measurement (d_1) has been chosen from 1 m to 4 m (0.5 m step). The number of rows (N_r) varies from 3 to 9. Finally, the number of columns (N_c) of every SC is fixed to 10, and the distance between the source and the center of the structure (d) is also fixed to 1.35 m.

By means of a random procedure, we have defined a set of 151 combinations of these parameters that produce 151 input vectors. Next, the corresponding experimental spectrum is measured for every vector. We have selected a sample of 145 of these pair vector-spectrum for ANNs learning process, and the remaining 6 pairs have been preserved to check the accuracy of the model (test).

B. MRA of the experimental spectra

Once we have obtained the experimental data, and before presenting them to ANNs, an adequate treatment is needed in order to simplify the information contained in them. As we have explained above, the mathematical tool chosen for doing that has been the MRA that allows us to: Divide the information contained in each spectrum into different resolution levels, filter each of these levels independently in order to delete noise, and compress all the information contained using a number of coefficients as smaller as possible to characterize the spectrum.

Attending to the shape of the peaks in the attenuation spectra, we have selected Daubechies 2 as the most convenient wavelet basis to perform the MRA analysis, since it allows one to represent attenuation peaks in a very accurate way with a very small set of coefficients. This can be seen in Fig. 3.

Now, we can perform the MRA of each spectrum up to the 9th wavelet level.

Once we have divided the information contained in each spectrum in different resolution levels, we can perform a filtering process which sets an independent threshold value for each level.

The final step is the reduction of the number of coefficients (compression of the information). To do that, we delete the two most detailed wavelet resolution levels. This does not affect the shape of the spectrum, although they represent a large number of coefficients (75% of the total). To illustrate this, Fig. 4 shows the reconstruction of a spectrum computing the inverse wavelet transform with only the remaining coefficients (25% of the total). As the reader can see, there is a remarkable coincidence between the reconstructed spectrum and the original one. In this sense, we obtain a high rate of compression of the spectra. For the MRA and the inverse wavelet transform, we have used the *Wavelet* MATLAB toolbox.²²

C. Design and training of the ANN

In our model, we have considered eight neural networks, one for each resolution level of the MRA analysis of experimental spectra, that work independently. The input in each of them is the parameter vector that determines the SC setup (input vector), and the output is a real-valued vector that

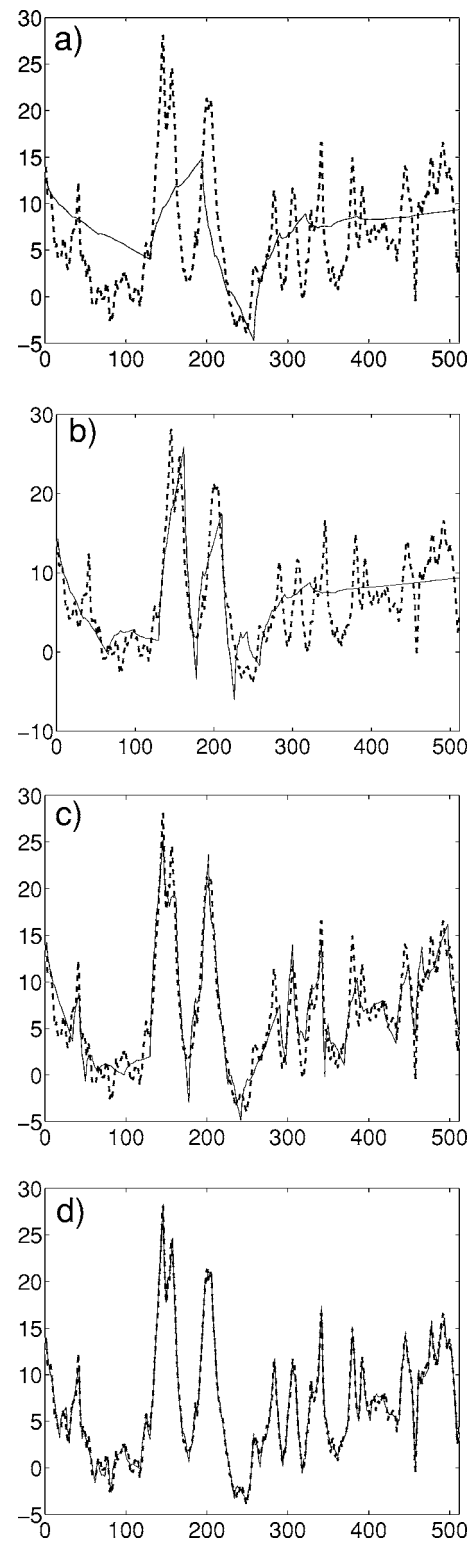


FIG. 3. Reconstruction of a typical experimental spectrum of 512 channels using (a) 5, (b) 10, (c) 30, and (d) 100 wavelet coefficients, respectively. The y axis represents the pressure attenuation in dB. The dashed line represents the reconstructed spectrum; and the continuous line, the original one.

gives us the wavelet coefficients of the simulated spectrum for the corresponding resolution level. Consequently, the main mathematical assumption is that every resolution level can be computed independently.

Due to the small size of the set of experimental spectra chosen, a simple neural network architecture is proposed: A

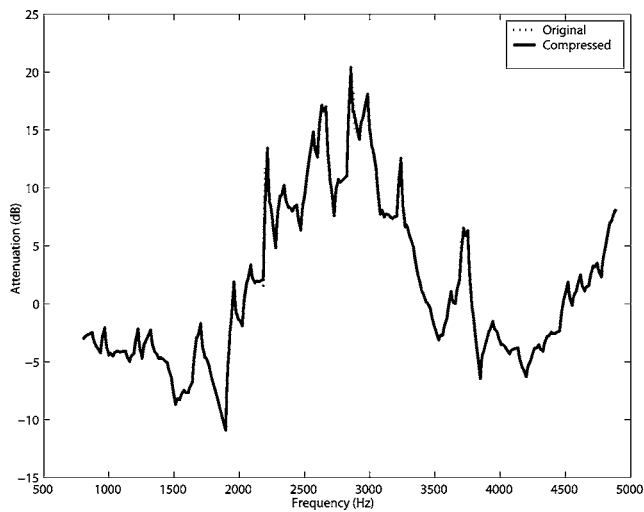


FIG. 4. Experimental spectrum versus its compressed version. It can be seen that the compressed versions cannot be distinguished from the original.

two-layer feedforward backpropagation network type. The first layer contains five neurons (the number of parameters that define the SC setup) with an \tanh activation function, and the second layer contains as many neurons as coefficients that have to be predicted with a \tanh activation function. This number varies depending on the MRA resolution level simulated by the neural network.

For the learning procedure, we feed the 8 networks with the experimental set of 146 inputs/outputs, and an optimization procedure of connection weights and bias is performed. At the very end, we have a final and optimal set of weights and bias for all networks. Then, the model is ready for simulating spectra: Giving to each neural network the same vector of parameters as input, they will return the wavelet coefficients corresponding to the MRA level assigned to each one. Computing the inverse wavelet transform of all of these coefficients together (all levels), we obtain the simulated spectrum associated with the SC setup encoded with this vector of parameters. For the effective computation of the model, we have used the *Neural Network* MATLAB toolbox.²¹

D. Test and results of the model

Once the ANNs have been trained, a test of the model must be performed. For this purpose, we have preserved six experimental spectra that have not been used for the training. In Fig. 5, we compare experimental and simulated spectra associated with three test SC setups.

The parameters corresponding to the simulated spectra are: Fig. 5(a): Incidence angle 5° cylinders radii 0.02 m, lattice spacing 0.0635 m, distance from the point of measurement to the center of the structure 4 m, and a number of rows 7; Fig. 5(b): Incidence angle 20° , cylinders radii 0.02 m, lattice spacing 0.0635 m, distance from the point of measurement to the center of the structure 2 m, and number of rows 6; and Fig. 5(c): Incidence angle 5° cylinders radii 0.0175 m, lattice spacing 0.0635 m, distance from the point of measurement to the center of the structure 4 m, and number of rows 9.

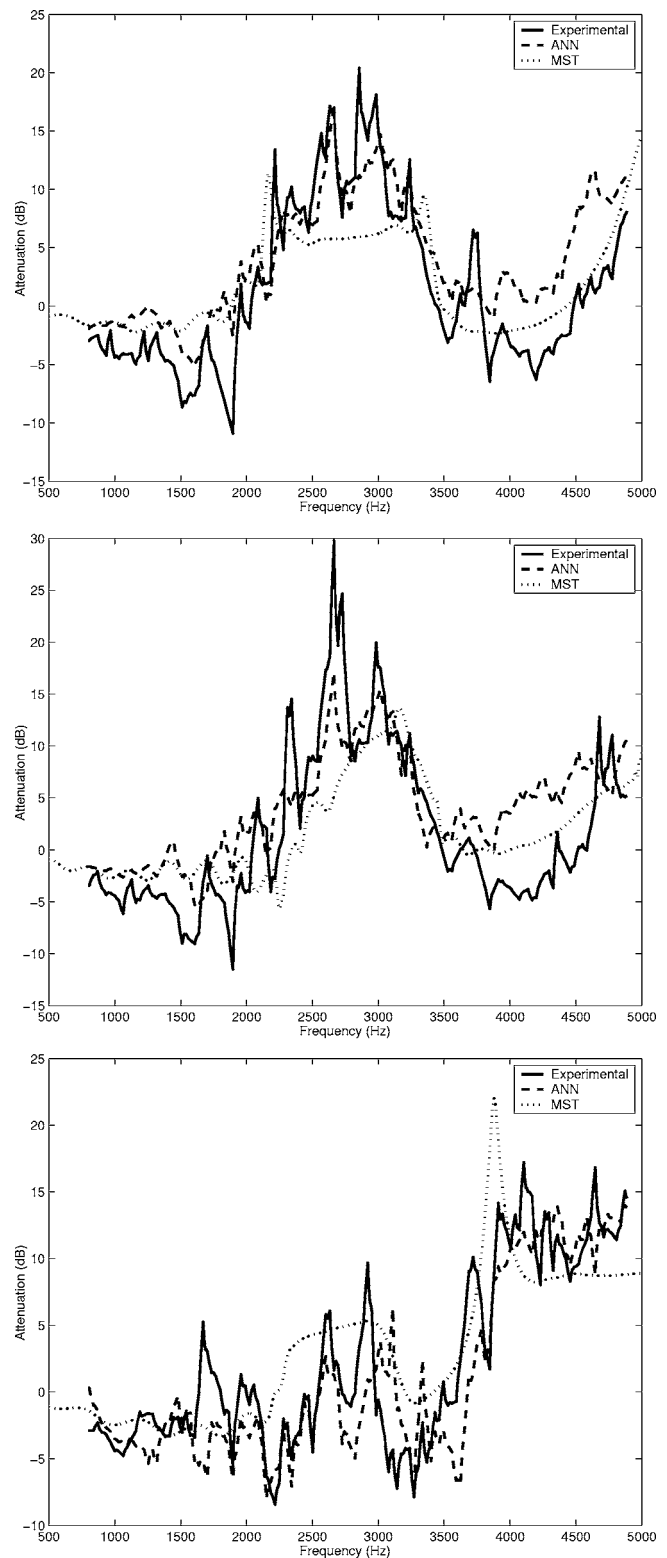


FIG. 5. Results of the test of the model for three of the test samples: Experimental spectra (continuous line), simulated spectra using our model (dashed line), and simulated spectra using MST (dotted line).

A very good agreement between simulation and experiment can be observed. Practically all simulated peaks in the whole spectrum have a correct centroid, width, and tail, i.e., the shape of the simulated spectrum is very similar to the experimental one. The simulated attenuation level is also in

TABLE I. Quadratic error values associated with the test spectra. In the second column, we show the errors associated with the MST predictions. The third column shows the errors associated with our model.

Test spectrum	ϵ_{MST}	ϵ_{ANNs}
1	2.54	1.96
2	4.42	4.24
3	6.28	4.71
4	7.22	4.45
5	8.48	5.08
6	7.7	3.4

good agreement with experimental data. There are no spurious peaks, that is, peaks that appear in the simulated spectra but are absent in the experimental ones.

1. Comparison with MST

The reason for choosing the SCs setup mentioned above is that it allows us to compare our model with the MST. In Fig. 5 (dotted line), we can see that—although MST provides a general representation of the tendencies of the experimental spectra—it does not perform a good prediction of the shape of the spectrum.

In order to quantify the accuracy of each model, we define a quadratic error by

$$\epsilon^2 = \frac{\sum_{i=1}^{512} [p_{theo}(f_i) - p_{exp}(f_i)]^2}{512}, \quad (1)$$

where we divide by the total number of channels (512). The results for the tests spectra are shown in Table I. The average errors are 6.11 dB for MST, and 3.97 dB for our model (35% smaller). As can be seen, our model reproduces the shape of the experimental spectrum and has an associated error smaller than the MST in all cases.

2. Dependence of the model on the training samples

To complete the test of the model, we analyze its dependence on the number of training samples. To do so, we have trained the ANNs with populations of 40, 80, and 146 spectra. In each case, we have obtained different weights for the ANNs connections, which produce different predicted spectra. In Fig. 6, we show the comparison between these predictions and the associated experimental spectra for one of the test spectra.

Looking at these results, and assuming that we want to work with simulated spectra with a correct shape and an error associated at least smaller than the one associated with MST, we are encouraged to use more than 100 training samples to build our model. But taking into account that we want to use a number of training samples, as small as possible in order to reduce the effort in the experimental measurements, we have arrived at a compromise of 146 training samples.

IV. CONCLUSIONS

In this paper, we have obtained a general procedure to simulate attenuation spectra generated by SCs exclusively

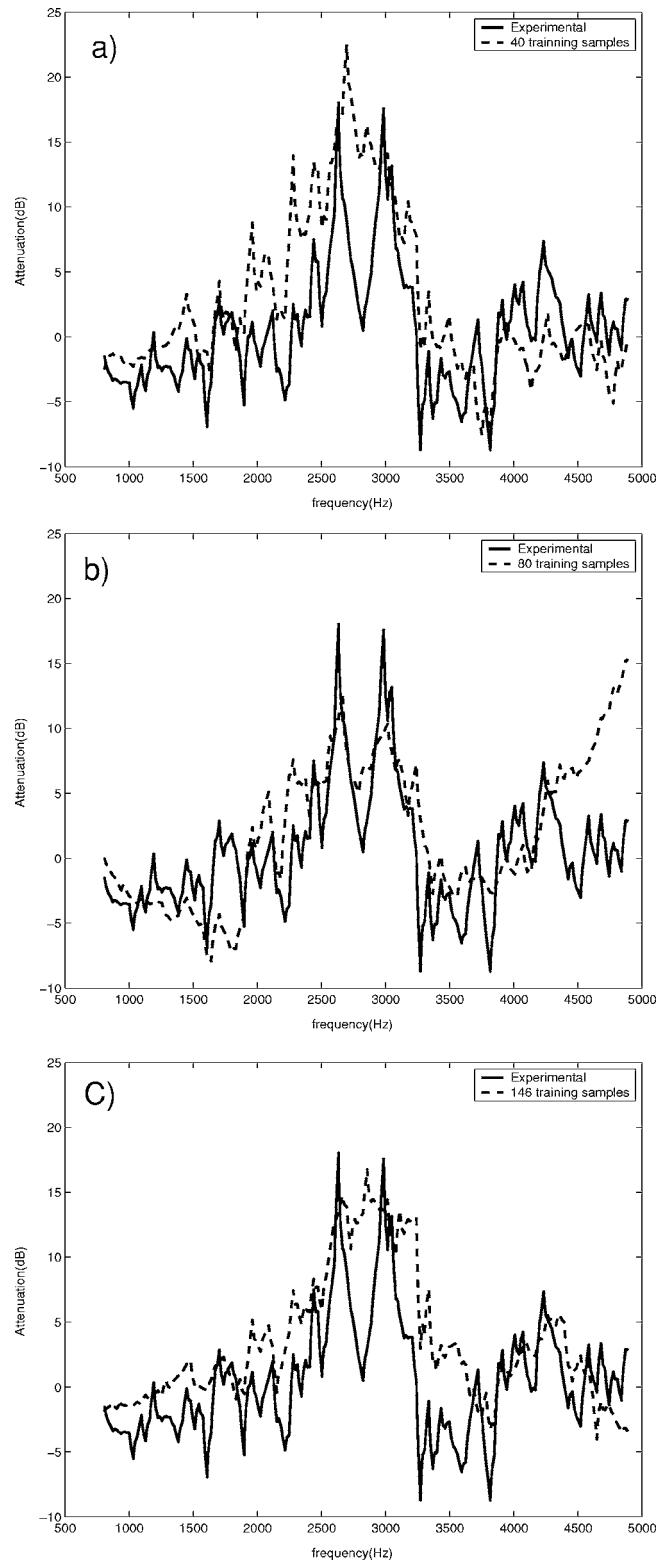


FIG. 6. Test spectrum obtained using a different number of training samples: (a) 40 training samples, (b) 80 training samples, and (c) 146 training samples.

based on experimental data, i.e., we have developed a phenomenological model of the behavior of SCs.

It is a general procedure that produces specific models, which effectively include the experimental conditions of measurements. This is an interesting property for technologi-

cal purposes. In this sense, the closer the experimental data to the technological situation where we want to use the SC, the more reliable the simulation.

In this case, we have used a simple experimental situation, where the MST applies, in order to compare it with our model. However, we want to remark that our model has the advantage of easy use in experimental situations, where other models cannot be used. For example, it can be used in the case of SCs with scatterers of complex geometry, or composed by materials of unknown acoustic impedance, or for any frequency range (ultrasound).

The training and learning of ANNs take a short time (a few minutes) and every simulation takes only a few seconds in a standard Pentium IV personal computer platform. Our procedure is extremely fast in comparison with other procedures based, for example, in multiple scattering. Once trained, it is very useful when combined with optimization technics (genetics algorithms).

The use of MRA based on wavelets, and the selection of an adequate basis, allows us to optimize the representation of the spectra via a small set of wavelet coefficients. We have been able to reduce 75% of the initial coefficients that characterize each spectrum without losing the main details.

Moreover, the combination of wavelet codification and a neural network structure allows us to construct a parallel computation model. The splitting of the signal into different resolution levels, that can be computed independently, makes it possible to divide a complex ANN that computes all spectra at the same time into eight simpler ANNs—all computing only one resolution level.

As a result of these two features mentioned above, a drastic reduction in experimental data needed for the training processes is possible. The fewer connections the ANNs have, the fewer experimental data are needed to adjust weights and bias.

We want to emphasize that this procedure can be used for other experimental goals that have an experimental spectrum associated as an output, such as the design of sound and ultrasound lenses, barriers, photonic crystals, and any filter device in general.

ACKNOWLEDGMENTS

This research has been partially supported by the Generalitat Valenciana (Spain), under Grant No. GV04B-371, by Comisión Interministerial de Ciencia y Tecnología of Spain, under Grant No. BFM2003-02302, and by Comisión Interministerial de Ciencia y Tecnología of Spain, Contract No. MAT 2003-04993-03.

The authors would like to thank the R+D+i Linguistic Assistance Office at the Universitat Politècnica de València, Aloma Domènech i Gamez, and Teba Olcina Rambla for their help in revising this paper.

- ¹R. Martínez-Sala, J. Sancho, J. V. Sánchez-Pérez, J. Llinares, and F. Meseguer, "Sound attenuation by sculpture," *Nature (London)* **378**, 241 (1995).
- ²J. V. Sánchez-Pérez, C. Rubio, R. Martínez-Sala, R. Sánchez-Grandía, and V. Gómez, "Acoustic barriers based on periodic arrays of scatterers," *Appl. Phys. Lett.* **81**, 5240–5242 (2002).
- ³A. Uris, C. Rubio, H. Estellés, J. V. Sánchez-Pérez, R. Martínez-Sala, and J. Llinares, "Design of lightweight multilayer partitions based on sonic crystals," *Appl. Phys. Lett.* **79**, 4453–4454 (2001).
- ⁴M. S. Kushwaha, "Stop-bands for periodic metallic rods: Sculptures that can filter the noise," *Appl. Phys. Lett.* **70**, 3218–3220 (1997).
- ⁵M. Shen and W. Cao, "Acoustic band-gap engineering using finite-size layered structures of multiple periodicity," *Appl. Phys. Lett.* **75**, 3713–3715 (2001).
- ⁶Y. Lai, X. Zhang, and Z. Zhang, "Engineering acoustic band gaps," *Appl. Phys. Lett.* **79**, 3224–3226 (2001).
- ⁷M. S. Kushwaha, P. Halevi, L. Dobrzynski, and B. Djafari-Rouhani, "Acoustic band structure of periodic elastic composites," *Phys. Rev. Lett.* **71**, 2022–2025 (1993).
- ⁸E. N. Economou and M. M. Sigalas, "Classical wave propagation in periodic structures: Cermet versus network topology," *Phys. Rev. B* **48**, 13434–13438 (1993).
- ⁹J. V. Sánchez-Pérez, D. Caballero, R. Martínez-Sala, C. Rubio, J. Sánchez-Dehesa, F. Meseguer, J. Llinares, and F. Gálvez, "Sound attenuation by a two-dimensional array of rigid cylinders," *Phys. Rev. Lett.* **80**, 5325–5328 (1998).
- ¹⁰M. Kafesaki and E. N. Economou, "Multiple scattering theory for 3D periodic acoustic composites," *Phys. Rev. B* **60**, 11993–11999 (1999).
- ¹¹M. M. Sigalas and N. Economou, "Attenuation of multiple-scattered sound," *Europhys. Lett.* **36**, 241–246 (1996).
- ¹²Y. Y. Chen and Z. Ye, "Theoretical analysis of acoustic stop bands in two-dimensional periodic scattering arrays," *Phys. Rev. E* **64**, 0366161–0366165 (2001).
- ¹³L. Sanchis, F. Cervera, J. Sánchez-Dehesa, J. V. Sánchez-Pérez, C. Rubio, and R. Martínez-Sala, "Reflectance properties of two-dimensional sonic band-gaps crystals," *J. Acoust. Soc. Am.* **109**, 2598–2605 (2001).
- ¹⁴O. Umnova, K. Attenborough, and C. Linton, "Effects of porous covering on sound attenuation by periodic arrays of cylinders," *J. Acoust. Soc. Am.* **119**, 278–284 (2006).
- ¹⁵I. Daubechies, *Ten Lectures on Wavelets* (SIAM, Philadelphia, 1999).
- ¹⁶L. Debnat, *Wavelets and signal processing* (Birkhauser, Boston, 2003).
- ¹⁷R. A. Devore and B. J. Lucier, *Wavelets*. *Acta Numerica*, edited by A. Iserles (Cambridge University Press, Cambridge, UK, 1992), Vol. **1**, p. 1.
- ¹⁸B. Kruse and B. Van der Smagt, *Introduction to Neural Networks* (University of Amsterdam, The Netherlands, 1996).
- ¹⁹M. T. Hagan, H. B. Demuth, and M. H. Beale, *Neural Network Design* (PWS, Boston, MA, 1996).
- ²⁰K. Levenberg, "A method for the solution of certain problems in least squares," *Q. Appl. Math.* **2**, 164–168 (1944).
- ²¹H. Demuth and M. Beale, *Neural Network Toolbox Users Guide* (The MathWorks, Inc., 1998).
- ²²M. Misiti, Y. Misiti, G. Oppenheim, and J. M. Poggi, *Wavelet Toolbox Users Guide* (The MathWorks, Inc., 2005).